INSTITUTE OF PHYSICS PUBLISHING SEMICONDUCTOR SCIENCE AND TECHNOLOGY
Semicond. Sci. Technol. **16** (2001) 372–376 www.iop.org/Journals/ss PII: S0268-1242(01)16570-3

Excess dark currents in HgCdTe p^+–n junction diodes

V Gopal[1], **S K Singh**[1] **and R M Mehra**[2]

[1] Solid State Physics Laboratory, Lucknow Road, Timarpur Delhi 110054, India
[2] Department of Electronic Science, University of Delhi South Campus, India

E-mail: VISHNU_GOPAL/SSPL@ssplnet.org

Received 22 August 2000, accepted for publication 15 January 2001

Abstract
This paper presents a result that shows that the trap-assisted tunnelling and band to band tunnelling mechanisms make negligible contributions to the dark current in an HgCdTe p^+–n junction. Alternatively, the excess dark current of these junctions can be fairly well accounted for by invoking the avalanche multiplication mechanism.

1. Introduction

In the last decade there has been considerable activity on the fabrication and study of p^+–n junctions in HgCdTe to realize high-performance detectors. Prior to this, IR detectors based on n^+–p junctions had dominated the research activity in HgCdTe. There are therefore numerous reported studies to understand the dark current behaviour of the n^+–p junction [1–3], but the origin of the excess dark current in p^+–n junctions is not well understood, as will be shown in this paper. Subsequently, an attempt is made to analyse the I–V characteristic of the HgCdTe p^+–n junction by invoking avalanche multiplication as one of the mechanisms contributing to the excess dark current of these diodes.

2. Dark current in the HgCdTe n^+–p/p^+–n junction

In the case of an ideal junction, the diffusion of thermally generated minority carriers constitutes the dark current. Any current in excess of the thermal diffusion current will be termed here as excess dark current. Previously, the excess dark current behaviour and the resultant dynamic resistance variation of n^+–p HgCdTe junction diodes has been interpreted by invoking: (i) trap-assisted tunnelling currents, wherein the traps in the depletion region or the traps in the quasi-neutral p-region close to the depletion region edge participate in the tunnelling process; (ii) band to band tunnelling currents; and (iii) surface leakage currents. In the first instance all of these current contributing mechanisms can also be thought of as possible mechanisms contributing to the dark current in p^+–n HgCdTe junction diodes. Consequently, the relevant expressions to calculate these dark currents in p^+–n junctions are given below.

2.1. Diffusion current (I_{dif})

The thermal diffusion of the minority carriers (i.e. electrons from the p-region and holes from the n-region) which constitute the dark current of an ideal p–n junction is described by the following well known equation [4, 5]:

$$I_{\mathrm{dif}} = \left[\frac{qAn_{\mathrm{i}}^2}{N_{\mathrm{a}}} \left\{ \frac{kT}{q} \frac{\mu_{\mathrm{e}}}{\tau_{\mathrm{e}}} \right\}^{\frac{1}{2}} + \frac{qAn_{\mathrm{i}}^2}{N_{\mathrm{d}}} \left\{ \frac{kT}{q} \frac{\mu_{\mathrm{h}}}{\tau_{\mathrm{h}}} \right\}^{\frac{1}{2}} \right] \times \left(\exp\left(\frac{qV}{kT} \right) - 1 \right) \quad (1)$$

where N_{d} is the donor concentration, N_{a} the acceptor concentration, n_{i} the intrinsic carrier concentration, A the junction area, V the diode bias voltage, τ_{e} the electron lifetime, μ_{e} the electron mobility, τ_{h} the hole lifetime and μ_{h} the hole mobility. The first term on the right-hand side of the above equation is the contribution of electrons from the p-side, while the second term is the contribution of holes from the n-side of the junction. In n^+–p and p^+–n junctions the contribution from the heavily doped side, being negligible, will be ignored.

2.2. Trap-assisted tunnelling current (I_{tat})

Let us first consider the trap-assisted tunnelling current of the electrons from the p-side of the junction. In this current, electrons may tunnel from the occupied trap states on the p^+-side or through trap sites present in the depletion region to the empty band state on the n-side of the junction [2–4]. Using a one-dimensional model, the current is given by

$$I_{\mathrm{tat}} = qAN_{\mathrm{t}}W_{\mathrm{dep}}W_{\mathrm{c}}N_{\mathrm{c}} \quad (2)$$

where N_{t} is the trap density, and W_{dep}, the depletion layer width, and $W_{\mathrm{c}}N_{\mathrm{c}}$, the tunnelling rate of electrons, are given

by [5–8]

$$W_{\rm dep} = \left[\frac{2\varepsilon_0\varepsilon_{\rm s}(V_{\rm bi}-V)(N_{\rm a}+N_{\rm d})}{qN_{\rm a}N_{\rm d}}\right]^{\frac{1}{2}} \tag{3}$$

$$W_{\rm c}N_{\rm c} = \frac{\pi^2 q m_{\rm e} E M^2}{h^3(E_{\rm g}-E_{\rm t})}\exp\left\{\frac{4(2m_{\rm e})^{\frac{1}{2}}(E_{\rm g}-E_{\rm t})^{\frac{3}{2}}}{(3q\hbar E)}\right\} \tag{4}$$

where ε_0 is the static dielectric constant, $\varepsilon_{\rm s}$ the dielectric constant of HgCdTe, $m_{\rm e}$ the electron effective mass, $E_{\rm g}$ the bandgap, h^3 the Planck constant, $E_{\rm t}$ the position of the trap in the bandgap measured from the top of the valence band on the p⁺-side and M the matrix element associated with the trap potential whose value is $(m_{\rm e}/m_0)M^2 = 10^{-23}$ V cm^3 [5–8]. E is the electric field strength of the depletion region, given by

$$E = \frac{(V_{\rm bi}-V)}{W_{\rm dep}} \tag{5}$$

$$E_{\rm t} = tE_{\rm f} = t\left[\frac{E_{\rm g}}{2} + \frac{kT}{q}\ln\left(\frac{m_{\rm h}}{m_{\rm e}}\right)^{\frac{3}{4}} - \frac{kT}{q}\ln\left(\frac{N_{\rm a}}{n_{\rm i}}\right)\right] \tag{6}$$

where $m_{\rm h}$ is the hole effective mass and t is a factor. For calculations we assume that $t = 0.7$ [2]. The trap-assisted tunnelling contribution from the n-side is ignored because donor activation energies are generally not observed in n-type HgCdTe material [9, 10].

2.3. Band to band tunnelling current ($I_{\rm btb}$)

Carriers tunnelling directly across the junction are responsible for the BTB current [1–3]. For modelling we use the simple approach presented in [1]. The band to band tunnelling current is given by

$$I_{\rm btb} = \frac{qA}{4\hbar\pi^2}\left\{\frac{E_{\rm g}kT}{P^2}\right\}^{\frac{1}{2}}\int_{-E_{\rm max}}^{0} T\left(\frac{E}{2}\right)\mathrm{d}E \qquad \text{where} \quad E_{\rm max} = -qV + E_{\rm f} \tag{7}$$

where P is the momentum matrix element and $E_{\rm f}$ the Fermi energy. $T_{\rm p}$, the tunnelling probability associated with the band to band tunnelling, is given by

$$T_{\rm p} = \exp\left[-\left(\frac{2m_{\rm e}}{\hbar^2}\right)^{\frac{1}{2}}\left(\frac{2\varepsilon_0\varepsilon_{\rm s}}{q^2N_{\rm d}}\right)^{\frac{1}{2}}E_{\rm g}\left\{\left(1-\frac{E}{E_{\rm g}}\right)\times\left[\frac{\pi}{2} - \sin^{-1}\left(\frac{-E}{E_{\rm g}-E}\right)^{\frac{1}{2}}\right] - \left(-\frac{E}{E_{\rm g}}\right)^{\frac{1}{2}}\right\}\right]. \tag{8}$$

Having outlined the various expressions above to estimate these dark currents, we now proceed to calculate these current components for an HgCdTe p⁺–n junction at temperature 78 K whose typical specifications are summarized in table 1. The individual current contributions are shown in figure 1. It can be clearly seen from this figure that the dark current of HgCdTe p⁺–n junctions will be dominated by the minority carrier (hole) diffusion current (■) from the n-side and that all other mechanisms, namely, diffusion of minority carriers (electrons) from the p⁺-side (●), trap-assisted tunnelling (∗) and band to band tunnelling (▼), make negligible contributions to the dark current. The minority carrier lifetimes used for the calculation of diffusion current in figure 1 are 10 ns (p-side) and 1 μs

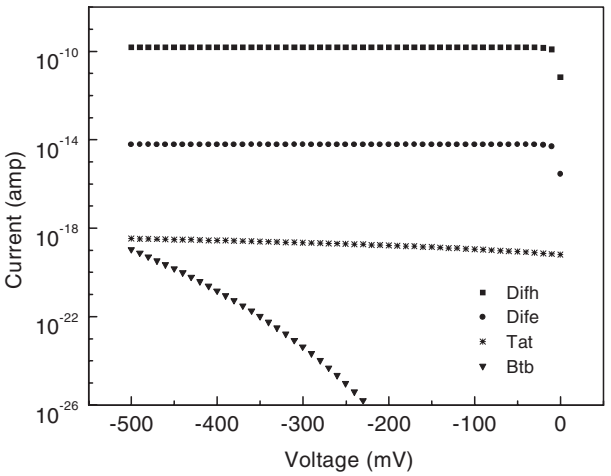

Figure 1. A comparison of dark current contributions due to thermal diffusion (■ and ● are contributions from n- and p-regions, respectively), trap-assisted tunnelling (∗) and band to band tunnelling (▼) in an HgCdTe p⁺–n junction.

Table 1. HgCdTe/Si diode parameters.

Composition x	0.25
Cutoff wavelength	8 μm
p-type carrier concentration	2×10^{18} cm^{-3}
n-type carrier concentration	1.7×10^{15} cm^{-3}
Junction area	2.5×10^{-5} cm^{-2}

(n-side). The trap density used for the calculation of the trap-assisted tunnelling current is 1×10^{15} cm^{-3}, which is generally reported in the literature [6, 7]. The reported data [11] on the HgCdTe p⁺–n junction diode however show that the reverse I–V characteristics and the resultant dynamic resistance–area product variation as a function of reverse bias voltage are very similar to that of n⁺–p junctions. This behaviour clearly indicates the presence of excess dark current contributions in p⁺–n junctions. Since neither of the current contributing mechanisms invoked in the case of the n⁺–p junction seem to explain the observation of excess dark current in the p⁺–n junction, we explore in this paper the possibility of an alternative mechanism, namely avalanche multiplication, as one of the possible mechanisms contributing to the excess dark current in HgCdTe p⁺–n junction diodes.

3. Avalanche multiplication

The dark current of a junction diode in which avalanche multiplication is assumed to be responsible for the excess dark current may be written as

$$I = M_{\rm d}(V)\, I_{\rm dif}. \tag{9}$$

In HgCdTe material the process of avalanche multiplication, once initiated, can be assumed to be dominated by the electron impact ionization [12] since (i) the impact ionization results in the production of electron–hole pairs and (ii) the threshold energy for the impact ionization of electrons is nearly half of that required for the hole impact ionization. The ratio of electron to hole ionization coefficients is 10 in 2.5 μm cutoff and should be even higher in the present case of LWIR HgCdTe

diodes [13]. The dark multiplication factor $M_d(V)$ in this case can be written as

$$M = \frac{1}{(1 - \alpha_e W_{dep})}. \tag{10}$$

In Shockley's 'lucky electron model', the electron impact ionization coefficient (α_e) is given by

$$\alpha_e = \frac{qE}{r\varepsilon_{ph}} \exp\left(-\frac{\varepsilon_i}{qEL_{ph}}\right) \tag{11}$$

where L_{ph} is the mean free path for phonon collisions, ε_i the threshold energy for the impact ionization (assumed to be equal to E_g), ε_{ph} the optical phonon energy (16 meV for the present case from [14]), r the relative probability of phonon emission to impact ionization for a hot electron and E the electric field across the depletion region.

However, it will be shown later in this paper that the reported data on the HgCdTe p^+–n junction diode can be fitted well, if the electron impact ionization coefficient (α_e) is assumed to be given by

$$\alpha_e = \alpha_0 \exp\left[-\frac{b}{E}\right]^m \tag{12}$$

where α_0 and m are empirical fitting parameters. The above form of the equation has been already shown to apply to other semiconductor materials such as Ge, Si and GaAs [15, 16].

4. Analysis of the experimental data

In this section we will analyse the reported [11] experimental I–V characteristic and the resultant dynamic resistance–area product variation as a function of reverse bias voltage in a p^+–n LWIR HgCdTe junction diode fabricated on HgCdTe epilayers grown on Si substrate. Since this is a wide-p^+ on narrow-n double-layer heterojunction (DLHJ), the minority carrier diffusion current of this diode can be modelled as analogous to a homojunction [17]. Furthermore, being an epitaxial diode, the diffusion current can be written as follows [18]:

$$I_{dif} = \left[\frac{qAn_i^2}{N_d}\left\{\frac{kT}{q}\frac{\mu_h}{\tau_h}\right\}^{\frac{1}{2}}\right] \tanh\frac{d}{L_p}\left(\exp\left(\frac{qV}{kT}\right) - 1\right) \tag{13}$$

where d is the thickness of the n-region. The above equation can be rewritten as

$$I_{dif} = \frac{kT}{qR_0}\left[\exp\left(\frac{qV}{kT}\right) - 1\right] \tag{14}$$

where R_0 is the zero-bias resistance. While analysing the result, and calculating the diffusion current of an ideal diode, we will use the experimental value of the R_0 read from the experimental dynamic resistance versus voltage curve. In this regard it may be noted that R_0 is the diffusion-limited zero-bias resistance as all other components contribute negligibly at zero bias.

Since this is a p^+–n junction, for all practical purposes the depletion width (where avalanche multiplication will take place) will be in the narrow n-region and therefore while calculating the multiplication parameter (α_e, M) the appropriate parameter corresponding to a narrow n-region has been used. The typical material/junction parameters required for this study are the same as summarized in table 1. The experimental I–V characteristic of the diode is shown in figure 3 by a continuous curve.

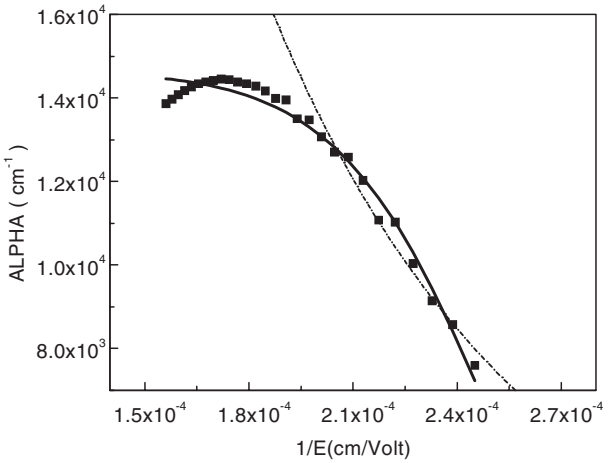

Figure 2. Impact ionization rate (■) as a function of reciprocal electric field calculated by assuming the source of excess dark current as impact ionization due to electrons in an HgCdTe p^+–n junction. The broken curve shows fitting to the lucky electron model equation (11) while the continuous curve shows fitting to equation (12).

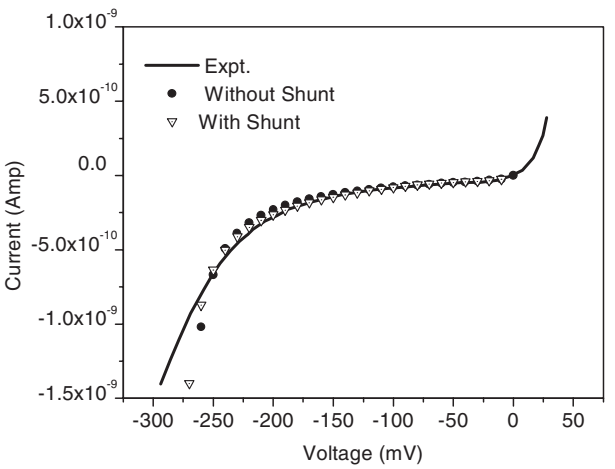

Figure 3. Comparison of the experimental (shown by a continuous curve) I–V curve as measured by Lyon *et al* [11] with the theoretical calculated one (shown by symbols ● and ▽). These curves were calculated by using equations (9) and (15) and the fitting parameters of HgCdTe listed in table 3.

The multiplication factor M and the ionization coefficient α_e as a function of electric field were calculated by dividing the experimentally measured current and the theoretically calculated diffusion current of an ideal junction using the model described above. A plot of α_e (thus calculated from the experimental data and shown by closed squares) as a function of the reciprocal electric field is shown in figure 2. It is observed that the shape of the α_e versus reciprocal electric field curve obtained here is in agreement with similar curves reported for several other semiconductor materials [15, 19]. When the experimental data on α were subjected to fitting to the lucky electron model equation (11), we obtained the broken

Table 2. Comparison of parameters obtained by fitting the lucky electron model.

Parameters	Present work	Miyatake *et al*	Elliot *et al*
L_{ph} (mean free path for phonon collisions) in μm	0.217	0.25 (8–10 μm) 0.02 (3–5 μm)	0.1 (8–12 μm)
r (relative probability of phonon emission for impact ionization)	5.3	40 (8–10 μm) 0.4 (3–5 μm)	20 (8–12 μm)

Table 3. Ionization rates in different semiconductors.

Semiconductors	α_0 (cm^{-1})	b (V cm^{-1})	m
Ge	1.55×10^7	1.56×10^6	1
Si	3.8×10^6	1.75×10^6	1
GaAs ⟨100⟩	9.12×10^4	4.77×10^3	3.48
⟨110⟩	2.19×10^6	2.95×10^6	1
⟨111⟩	7.76×10^4	4.45×10^5	6.91
HgCdTe (present work without shunt)	1.46×10^4	3.93×10^3	9.3
HgCdTe (present work with shunt)	1.45×10^4	4.65×10^3	13.9

curve shown in figure 2. A comparison of the corresponding best fit parameters L_{ph} and r in this paper with the earlier reported values (shown in table 2) suggests that our estimates of α are reasonable. Next it is observed that the lucky electron model fits to the data only at low electric field. However a much better fit (continuous curve) to the calculated data can be obtained by using equation (12). The value of the fitting parameter, α_0, b and m are shown in table 3 along with the corresponding values reported in the literature for other common semiconductor materials [15, 16].

5. Discussion

A comparison of the theoretically generated I–V curve (shown by symbol ●) using the fitting parameters listed in table 3 and equation (9) with the experimental data is shown in figure 3. Figure 4 shows the comparison of the variation of dynamic resistance–area product as a function of voltage. The curves represented by the discrete points and continuous curve, respectively, correspond to theoretical and experimental I–V curves shown in figure 3. It is clearly observed that the experimental I–V characteristic as well as the resultant dynamic resistance–area product variation can be fairly well accounted for by invoking the avalanche multiplication mechanism in the p$^+$–n HgCdTe junction. Disagreement between experiment and theory is, however, observed in the relatively high-bias region in both I–V and R_d–V characteristics. In addition, a notable disagreement is visible between the calculated peak dynamic resistance and the experimental value in figure 4, though good agreement is seen in the I–V characteristics shown in figure 3. One of the possibilities for this kind of observation could be the result of overestimating the avalanche multiplication. This could happen if the experimental I–V characteristic includes an ohmic surface leakage current component beside the diffusion current component. The former current, being simply responsible for a shunt resistance effect, would not undergo avalanche multiplication. In other words, equation (9) would then be applicable in the following

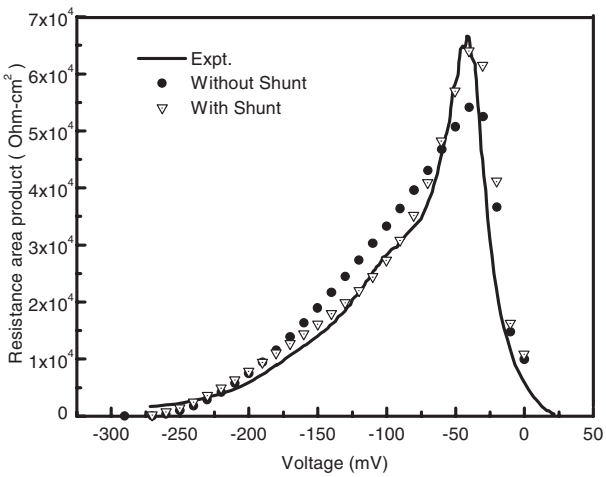

Figure 4. Comparison of experimentally observed and theoretically calculated (shown by symbols ● and ▽) variation of dynamic resistance–area product in reverse bias. These curves were obtained by differentiating the respective curves shown in figure.

modified form:

$$I = M_d(V) I_{dif} + \frac{V}{R_s}. \tag{15}$$

Analysis of the experimental data by using the above equation in place of equation (9) leads to excellent agreement (shown by symbols ▽) between theory and experiment in both I–V and R_d–V characteristics.

6. Conclusions

It is concluded that the excess dark current in LWIR HgCdTe p$^+$–n junction diodes cannot be accounted for by trap-assisted tunnelling and band to band tunnelling mechanisms. Instead it can be interpreted by invoking the avalanche multiplication mechanism and the fact that the process of avalanche multiplication in HgCdTe junction diodes is dominated by the impact ionization of electrons.

Acknowledgment

The authors (VG and SKS) are grateful to Professor Vikram Kumar, Director, Solid State Physics Laboratory, Delhi, for constant encouragement and granting permission to publish this paper.

References

[1] Nemirovsky Y, Rosenfeld D, Adar R and Kornfeld A 1989 *J. Vac. Sci. Technol.* A **7** 528–35
[2] Nemirovsky Y, Fastow R, Meyassed M and Unikovsky A 1991 *J. Vac. Sci. Technol.* B **9** 1829–39
[3] Singh S K, Gopal V, Bhan R K and Kumar V 2000 *Semicond. Sci. Technol.* **15** 752–5
[4] Rogalski A 1988 *Infrared Phys.* **28** 139–53
[5] Wong J Y 1980 *IEEE Trans. Electron Devices* **27** 48–57
[6] Nemirovsky Y and Unikovsky A 1992 *J. Vac. Sci. Technol.* B **10** 1602–10
[7] Rosenfeld D and Bahir G 1992 *IEEE Trans. Electron Devices* **39** 1638–45
[8] Reine M B, Sood A K and Tredwell T J 1981 *Photovoltaic Infrared Detectors, Semiconductors and Semimetals* vol 18, ed R K Willardson and A C Beer (New York: Academic) chapter 6
[9] Rogalski A, Jozwikowska A, Jozwikowska K and Rutkowski J 1993 *Semicond. Sci. Technol.* **8** S289–92
[10] Ciupa R, Rogalski A, Rutkowski J and Piotrowski J 1994 *SPIE* **33** 1434–8
[11] Lyon T J de, Rajavel R D, Jensen J E, Wu O K and Vigil J A 1996 *SPIE* **2816** 29–41
[12] Capper P 1997 *Narrow-Gap II–VI Compounds for Optoelectronic and Electromagnetic Applications* (London: Chapman & Hall) ch 15, pp 450–73
[13] Elliot C T, Gordan N T, Hall R S and Crimes G 1990 *J. Vac. Sci. Technol.* A **8** 1251–2
[14] Miyatake T, Sugiyama I, Kajihara N and Miyamoto Y 1997 *SPIE* **3061** 68–77
[15] Shur M 1990 *Physics of Semiconductor Devices* (Englewood Cliffs, NJ: Prentice-Hall)
[16] Tyagi M S 1991 *Introduction to Semiconductor Materials and Devices* (New York: Wiley)
[17] Kraut E A 1989 *J. Vac. Sci. Technol.* A **7** 420–3
[18] Gopal V 1997 *Int. J. Electron.* **83** 191–200
[19] Pearsall T P 1978 *Solid-State Electron.* **21** 297–302